

Fundamentals and Applications of Electron Holography

Akira Tonomura

Advanced Research Laboratory, Hitachi, Ltd.

Advanced Science Institute, RIKEN

Japan

1. Introduction

Electron holography is a two-step imaging method devised by D. Gabor (Gabor, 1949): an electron hologram is formed as an interference pattern between an object wave and a reference wave, and the object electron wave is reconstructed as an optical wave by illuminating a laser beam onto hologram film. The reconstruction has been facilitated by advances in digital reconstruction techniques. The reconstructed optical wave is similar to the original object electron wave except for the scale ratio of the electron and light wavelengths, and it represents the “wavefunction” of the object electron wave.

Gabor intended to optically compensate for the aberrations in the electron lens system, a factor limiting the resolution of electron microscopes. Thanks to the development of bright and yet coherent field-emission electron beams, electron holography proved to be useful not only for high resolution microscopy but also for phase microscopy at the level of atoms and molecules (Tonomura, 2005). The wavefronts of electrons transmitted through an object contain information about the object's shape and size and also about the electromagnetic fields inside and outside the object. Furthermore, since the wavelengths of fast electrons are extremely short, such as 0.009 Å for 1-MV electrons, the wavefronts can be observed with high spatial resolution. The interaction of an electron wave with electromagnetic fields is described by the Aharonov-Bohm (AB) effect (Aharonov & Bohm, 1959). The AB effect principle has been used to observe not only quantum phenomena but also the microscopic distributions of electromagnetic fields by measuring the phases of electrons. The behavior of vortices in superconductors has also been observed by Lorentz microscopy as well as by interference electron microscopy.

This chapter describes fundamental experiments in quantum mechanics and the application results of electromagnetic field observation using electron holography. These experiments include the observation of magnetic heads for perpendicular recording, of Josephson vortices in YBCO thin film, and of the nucleation of the ferromagnetic phase assisted by magnetic fields in colossal magnetoresistance.

2. Interaction of electrons with electromagnetic fields – the Aharonov-Bhom effect –

In electron holography, electron wavefronts, or “electron wavefunctions”, are reconstructed. Therefore, we first discuss the interaction of incident electron waves with electromagnetic

fields. In classical mechanics, electrons passing through electromagnetic fields are deflected by Lorentz forces. In quantum mechanics, electrons propagate as waves, and their behavior is explained by the Schrödinger equation. In that realm, the concept of force is no longer relevant: electric field \mathbf{E} and magnetic field \mathbf{B} , defined as forces acting on a unit charge, take on a secondary meaning. Instead of forces, “phase shifts” come into play. The primary physical entities are neither \mathbf{E} nor \mathbf{B} but electrostatic potential V and vector potentials \mathbf{A} since phase shifts are produced by these potential, as described by the Schrödinger equation. In 1959, Y. Aharonov and D. Bohm theoretically predicted that a relative phase shift is produced by the potentials and can be observed as a displacement of interference fringes even when electrons pass through spaces free of \mathbf{E} and \mathbf{B} . This effect was later dubbed “the Aharonov-Bohm (AB) effect”.

The AB effect increased in significance in the late 1970s in relation to the theories attempting to unify all fundamental interactions in nature, in which potentials are extended to “gauge fields” and regarded as the most fundamental physical quantity. T. T. Wu and C. N. Yang (Wu & Yang, 1975) stressed the significance of the AB effect in relation to the physical reality of gauge fields.

Soon after the theoretical prediction of the AB effect, experimental testing was carried out. The first experiment was conducted by R. G. Chambers (Chambers, 1960) in 1960 (Fig. 1(a)). He placed a tapered iron whisker in the shadow of a biprism filament and detected a phase difference between two electron waves passing on both sides of the biprism though magnetic fields leaking out from the whisker and thus influencing incident electrons. The value of the phase difference was determined by the magnetic flux enclosed by the two waves, exactly as predicted by the AB effect. Other experiments followed: Fowler *et al.* (Fowler *et al.*, 1961) used a uniform iron whisker as a biprism filament (Fig. 1(b)). Boersch *et al.* (Boersch *et al.*, 1962) used a permalloy thin film evaporated on the bottom of a biprism filament (Fig. 1(c)). Möllenstedt and Bayh (Möllenstedt & Bayh, 1962) made a beautiful experiment using a tiny solenoid with a diameter as small as 1 μm .

They all detected the phase difference predicted by the AB effect. However, vector potentials have long been regarded as mathematical auxiliaries, so some people questioned the existence of the AB effect, thus causing a long controversy (Bocchieri & Loinger, 1978; Peshkin & Tonomura, 1989). The reported results were attributed by the opponents of the AB effect to the effect of magnetic fields leaking out from both ends of the finite solenoids or ferromagnets used in the experiments (Bocchieri & Loinger, 1981; Roy, 1980).

3. Conclusive experiments for the AB effect

An infinitely long magnet cannot be obtained experimentally, but an ideal geometry can be achieved in a finite size by using a toroidal magnet.

We first fabricated a leakage-free tiny magnet made of permalloy with a square-toroid geometry (Tonomura *et al.*, 1982) (Fig. 2) and detected a non-zero phase difference between two electron waves passing inside the hole and outside the toroid (Fig. 2(b)). However, this finding was not accepted by everyone, and papers were published disagreeing with our conclusion (Bocchieri *et al.*, 1982; Miyazawa, 1985). They argued that, to prove the AB effect, the electrons should not touch the magnetic field. They claimed that since the detected phase difference could not be due to ‘vector potentials’, magnetic fields (although slight) leaked out from even our ‘square’ toroidal magnets, mainly due to the existence of corners in the square sample (Tonomura, 1983) (Fig. 2(c)), so that part of the electron waves touched and even penetrated the magnet (Fig. 2(a)).

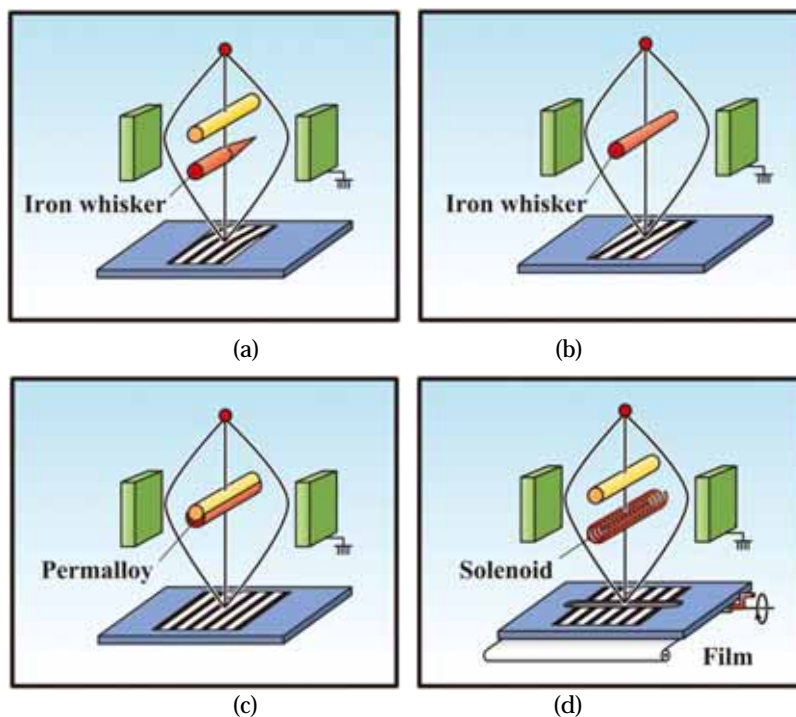


Fig. 1. Experimental arrangements for testing the AB effect in 1960s. (a) Chambers placed a tapered iron whisker in the shadow of a biprism filament, (b) Fowler *et al.* used a uniform iron whisker as a biprism filament, (c) Boersch *et al.* evaporated ferromagnetic permalloy on the bottom of a biprism filament, (d) Möllenstedt and Bayh placed a tiny solenoid in the shadow of a biprism filament. Tiny ferromagnets or solenoids with finite lengths were used for testing in these experiments. Later in the '80s, the existence of the AB effect was questioned because magnetic fluxes leaked out from both ends of the finite solenoids or magnets.

We thus carried out further experiments using a 'circular' toroidal magnet having even smaller leakage flux (Tonomura *et al.*, 1983) (Fig. 3(a)) and again detected the AB phase difference. To present the overlap of incident electrons with the magnetic field inside the sample, we next conducted experiments using a 'circular' toroidal magnet on top of which a thick gold film was evaporated (Tonomura *et al.*, 1984), which prevented electron penetration into the magnet (Fig. 3(b)). In this experiment, however, we could not determine the absolute value of the phase difference between the two electron beams, only their fractions in units of 2π . The obtained interference pattern (Fig. 3(b)) indicates that the interference fringes inside the hole and outside the toroid were not aligned, thus providing evidence for the AB effect even when incident electrons do not penetrate the magnet. Skeptics, however, asserted that the toroidal magnet should not only be covered on its top surface but also be fully covered on all its surfaces since the tail of the electron wavefunction curls around the sample and touches the magnetic field.

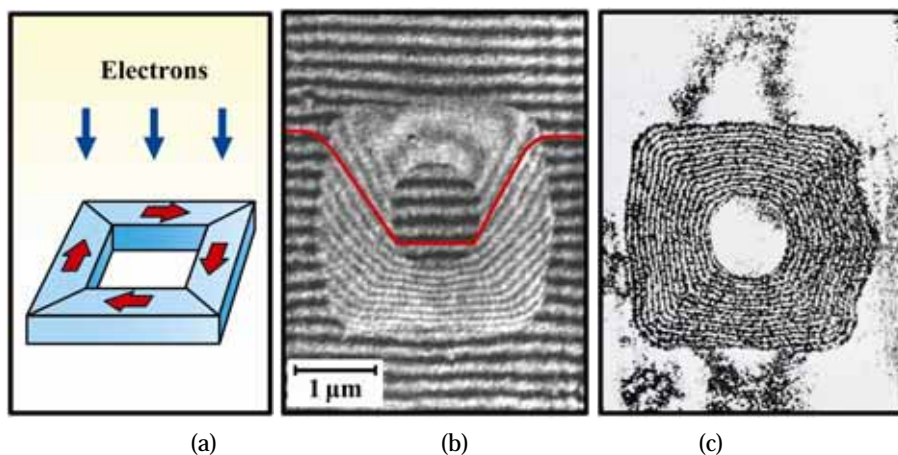


Fig. 2. Experiments using square toroidal magnet. (a) Schematic. (b) Interference pattern showing relative phase difference of $7 \times (2\pi)$ between inside and outside toroid. (c) Flux leaking from toroidal magnet. Toroidal ferromagnetic samples were used to minimize leakage flux. Contour lines of transmitted electron wavefronts indicate magnetic lines in magnetic flux units of h/e , confirming that the amount of leakage flux was approximately 1/15 of total flux, $h/2e$, since the phase difference was amplified by a factor of 2.

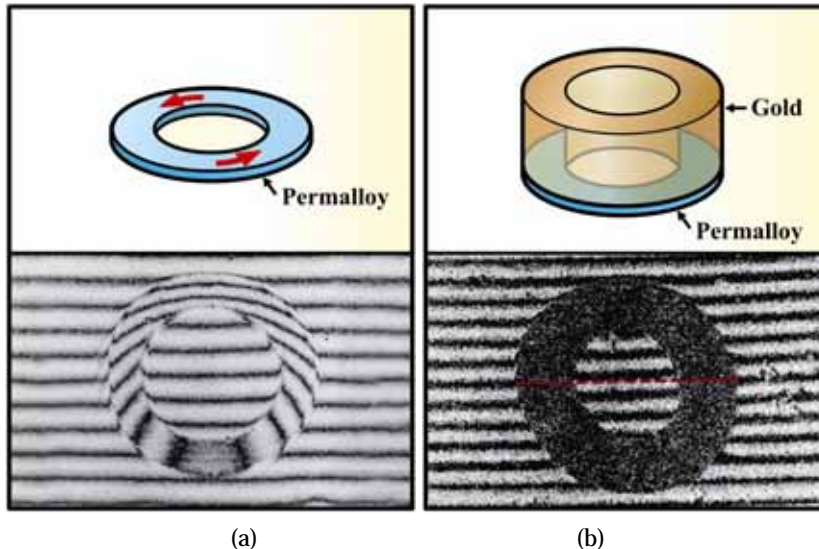


Fig. 3. Circular toroidal magnets made of permalloy. (a) Transparent toroidal magnet (permalloy film 10 nm thick). (b) Opaque toroidal magnet covered with gold film (permalloy film 10 nm thick; gold film 300 nm thick).

According to this challenge, we fabricated tiny toroidal magnets completely surrounded by superconductors (Tonomura *et al.*, 1986), thereby removing any ambiguities about the leakage flux and also about the overlap of incident electrons with the magnetic field in the solenoid or magnet. A permalloy toroidal magnet was completely covered with a niobium superconductor to confine the magnetic flux within the sample (Figs. 4(a) and (b)). The AB phase difference was again detected (Fig. 4(c)) even though magnetic field leakage was prevented by the Meissner effect, and the electrons did not touch the magnetization inside the sample.

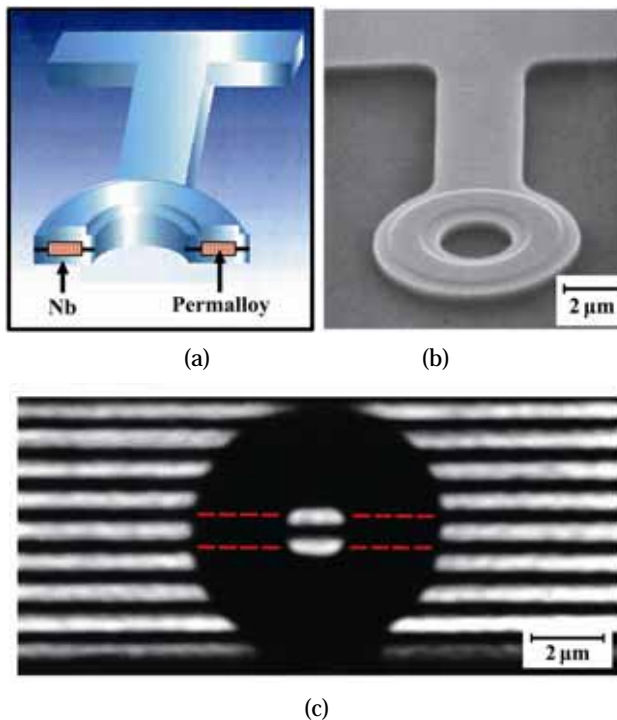


Fig. 4. Conclusive experiment proving existence of the AB effect using toroidal magnet completely covered with superconductor. (a) Schematic. (b) Scanning electron micrograph of sample. (c) Interference pattern at $T = 5$ K. Toroidal ferromagnetic permalloy sample was covered with Nb layers. Leakage magnetic fluxes were confirmed by electron holography to be less than $1/20$ of total magnetic flux passing through permalloy magnet. When sample temperature was decreased below superconductive critical temperature of Nb 9.2 K, the phase difference between two electron beams passing through inside the hole and outside the sample was quantized in π units, either zero or π . This magnetic flux quantization in $h/2e$ units proves that the magnetic fluxes were completely confined within the sample due to the Meissner effect. The production of a phase difference of π under the condition of no overlap of electrons and magnetic fields confirmed the AB effect.

We fabricated many toroids, more than 100,000 of different sizes having different magnetic flux values thanks to advances in lithography (Fig. 5), but obtained only two phase-shift values. The detected phase difference value was either π or 0. The phase-shift quantization in π units, indicating the magnetic flux quantization in superconductors, confirmed the complete covering of the magnetic flux within the superconductor, so flux leakage was prevented by the Meissner effect. In addition, the toroidal samples were covered with additional Cu layers so that incident electrons could not penetrate them and touch the magnetic field inside. Therefore, the results shown in Fig. 4(c) decisively confirmed the AB effect.

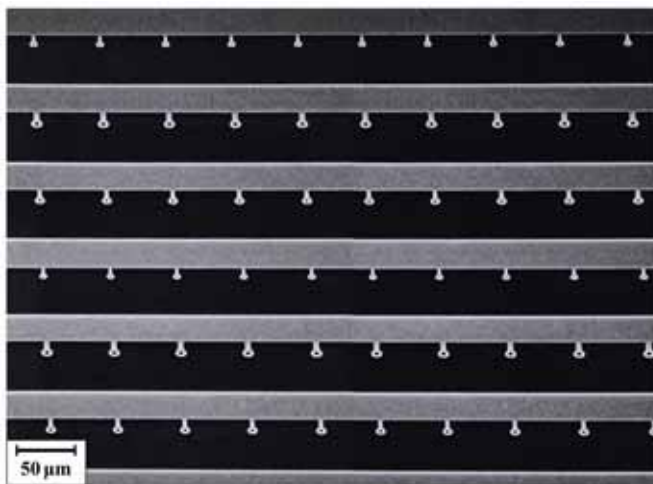


Fig. 5. Scanning electron micrograph of array of toroidal magnets covered with superconductors. More than 100,000 various samples were fabricated photolithographically.

4. Applications of electron holographic interferometry

We found in 1980 that quantitative magnetic lines of force can be visualized using the AB effect principle (Tonomura *et al.*, 1980). An example of a hexagonal cobalt particle is shown in Fig. 6. With electron microscopy, only its outline can be observed (Fig. 6(b)). With interference microscopy, however, circular phase contour fringes can be observed inside the particle (Fig. 6(c)). These fringes in the interference micrograph, phase-amplified two times, directly indicate quantitative magnetic lines in $h/2e$ flux units irrespective of the velocity of incident electrons. This results from the AB effect. The phase difference between two electron beams passing through two points in the specimen plane is determined by the magnetic flux enclosed by the two beam paths: a phase difference of 2π is produced by a magnetic flux of $h/e = 4.1 \times 10^{-19}$ Wb. Therefore, when two points in the specimen plane lie on a magnetic line, no phase difference is produced. That is, phase contour lines indicate magnetic lines of force. When the two electron beams enclose a magnetic flux of h/e , a phase difference of 2π is produced. That means phase contour fringes appear every h/e flux units. This observation principle is the same as that of a SQUID.

Not only magnetic fields but also electric fields can phase-shift incoming electrons. In fact, electrons entering a non-magnetic sample are accelerated by inner potential V_0 of the

materials, so their wavelength is shortened, as shown in Fig. 7(a). Therefore, the wavefronts inside the specimen are delayed proportional to the specimen thickness. The wavefront displacements cannot be observed in an electron micrograph (Fig. 7(b)), but can be observed in an interference micrograph (Fig. 7(c)) as displacements from regular fringes. The displacements indicate thickness contours in 20 nm thickness units.

An example of a triangular cobalt particle affected by both magnetic lines and sample thickness is shown in Fig. 8. A thickness contour map forms on the periphery (Fig. 8(b)) while circular magnetic lines form in the inner region since the sample thickness is uniform.

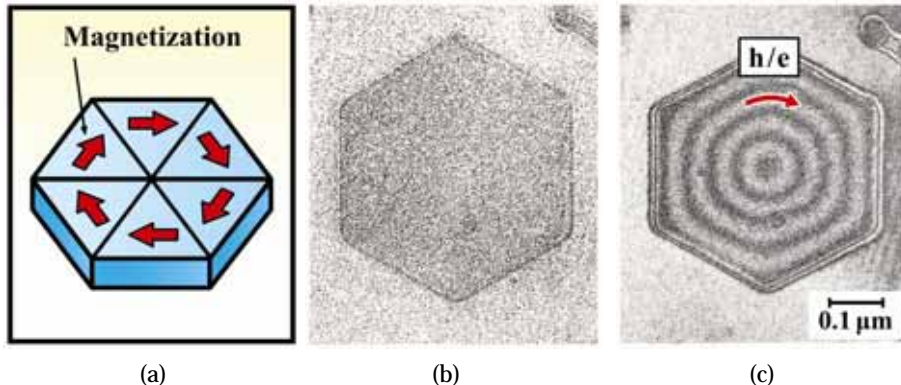


Fig. 6. Hexagonal cobalt particle. (a) Schematic. (b) Electron micrograph. (c) Interference micrograph (phase amplification $\times 2$). Phase contours in interference micrograph (c) indicate magnetic lines in $h/2e$ flux units. Magnetic lines are circular inside the particle.

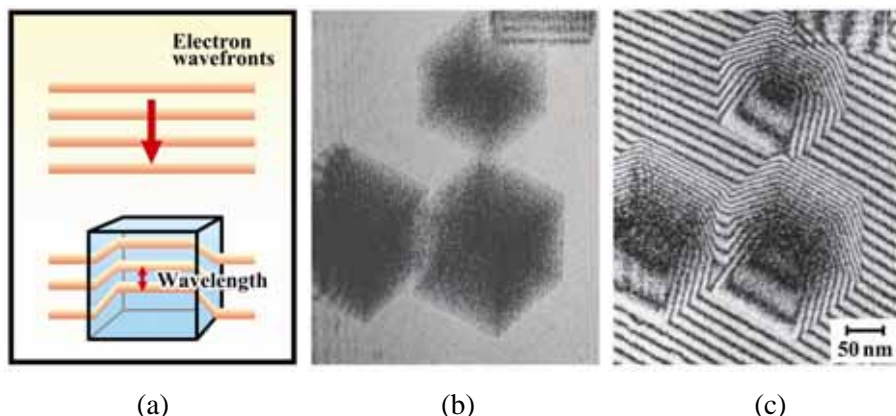


Fig. 7. Magnesium-oxide particle. (a) Schematic of wavefronts penetrating non-magnetic sample. (b) Electron micrograph. (c) Interference micrograph (phase amplification $\times 2$). Electrons are accelerated by inner potential V_0 , and their wavelength shortens as illustrated in (a). Although only the outlines of the particles are observed in the electron micrograph (b), thickness contours in units of 20 nm are observed as deviations from regular interference fringes in the interference micrograph (c).

A more practical application of electron holographic interferometry to “in-plane” magnetic recording (Osakabe *et al.*, 1983) is shown in Fig. 9. A magnetic head slides across a metal tape, and the bit patterns are recorded. The observed magnetic lines below are exactly like a stream of water since we are looking at a divergence-free \mathbf{B} . We can see that, where two streams of magnetic lines collide head on, vortices are produced. The magnetic lines meander toward the edge of the tape and then beyond the tape edge.

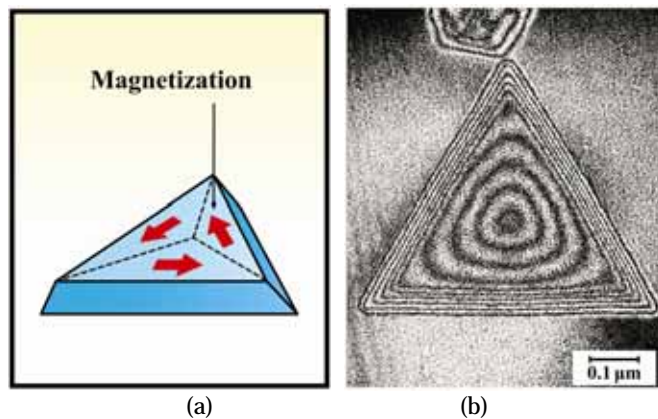


Fig. 8. Triangular cobalt particle. (a) Schematic. (b) Interference micrograph (phase amplification $\times 2$). Phase contours in peripheral part of particle in (b) indicate thickness contours, and those in central part indicate in-plane magnetic lines.

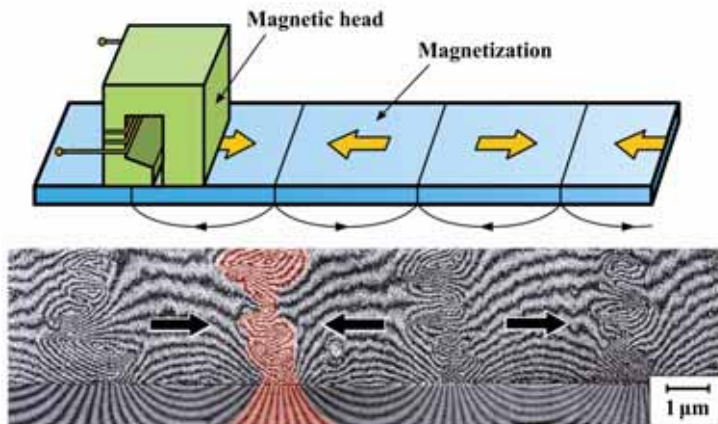


Fig. 9. Magnetic lines inside and outside a recorded magnetic tape. Detailed magnetic lines observed under various conditions, such as tape material and spacing and gap of head, provide information about how higher density recording can be attained.

The performance of a magnetic head has been investigated by electron holography (Kim *et al.*, 2008). Magnetic lines from a tiny magnetic head for “perpendicular” high-density

recording are evident in Fig. 10(a). While a high and localized magnetic field is needed, other characteristics are also required. For example, we also have to be able to control the head in any way we want. In some cases, we need to get a zero field outside the head, which is not easy since the density of magnetic lines inside ferromagnets remains constant.

For specific head materials and shapes, magnetic fields leaking from the head become negligible when the applied magnetic field is removed: straight magnetic lines inside the head (Fig. 10(a)) change into “U-turn” lines (Fig. 10(b)). At the pole tip, the magnetic lines form a tiny closed circuit. This remanent state in Fig. 10(b) is reversible, but slightly history-dependent (Hirata et al., 2009), as shown in Figs. 11(a) and (b).

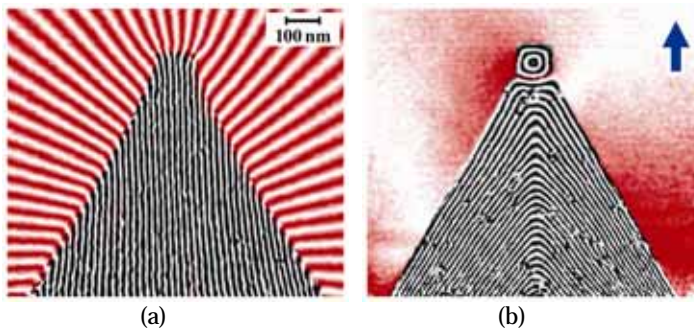


Fig. 10. Magnetic lines of magnetic head for perpendicular recording. (a) Magnetized state ($\mathbf{H} = 150$ Oe). (b) Remanent state ($\mathbf{H} = 0$ Oe). Magnetic lines from magnetic head provide direct information about recording magnetic lines when magnetic field \mathbf{H} is applied and also about leakage magnetic lines.

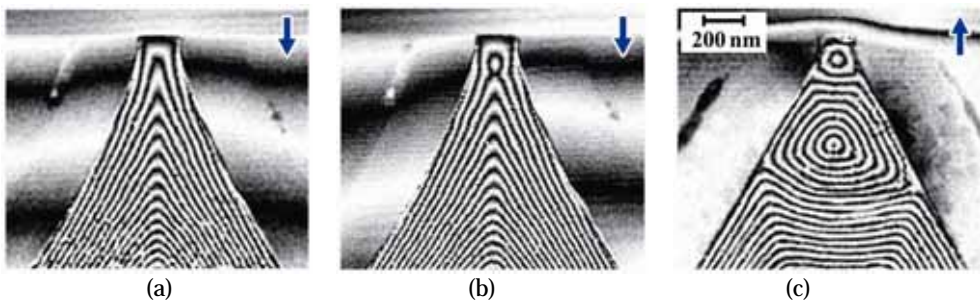


Fig. 11. Different remanent states of magnetic heads. (a) Magnetic lines of NiFe head when magnetic field applied in upward direction was removed. (b) A little different magnetic lines though under the same condition as (a). (c) Magnetic lines of NiFeCo when magnetic field applied in upward direction was removed. Remanent states are important since leaking magnetic flux sometimes erases recorded magnetic information.

We also found that the remanent pattern depends on the material. When the head material was changed from “nickel-iron” to “cobalt-nickel-iron”, the remanent state became irreversible, and the remanent pattern greatly changed (Hirata et al., 2009). An example is shown in Fig. 11(c): a large closure domain was produced in addition to the smaller one.

A more recent application example is the observation of the nucleation and growth of ferromagnetic domains in colossal magnetoresistance (CMR) materials (Murakami *et al.*, 2009). In CMR, an electric current begins to flow when the magnetic field increases or the temperature decreases. The microscopic mechanism for this is explained as follows: isolated tiny ferromagnets nucleate and coalesce in the ‘insulating’ phase, thus creating conduction paths for electrons. Using Lorentz microscopy, we investigated how this happens microscopically. When we reduced the sample temperature, a tiny spot suddenly appeared with bright and dark contrast features. The single magnetic domain (Fig. 12(a)) changed after a tremor into a double domain (Fig. 12(b)) and grew, keeping the double-domain form for a while (Fig. 12(c)) since these states are energetically stable. The double domains then coalesced into multiple domains (Fig. 13), until finally expelling insulating domains.

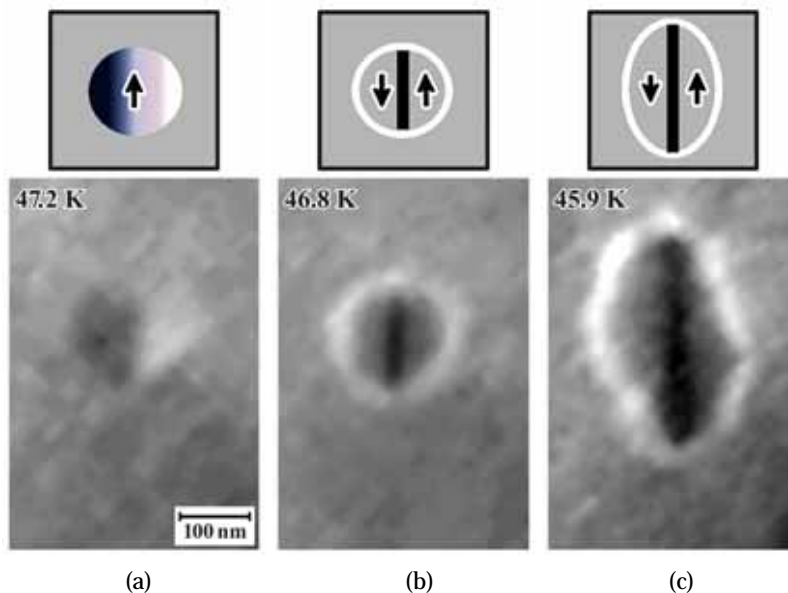


Fig. 12. Lorentz micrographs of $\text{La}_{0.25}\text{Pr}_{0.375}\text{Ca}_{0.375}\text{O}_3$ thin film. (a) Single domain at $T = 47.2$ K. (b) Double domain produced immediately after magnetization reversal at $T = 46.8$ K. (c) Growing double domain at $T = 45.9$ K.

We found two kinds of “boundaries”, straight and zigzag. The domain walls inside the ferromagnetic phase were smooth, while the boundaries between the ferromagnetic and insulating phases were zigzag. We concluded that, in the insulating domains, there must exist tiny charge-ordered clusters that cannot easily become ferromagnetic. The boundaries between ferromagnetic and insulating domains are affected by these clusters, resulting in zigzag boundaries and their stepwise motion. The boundaries between the two ferromagnetic domains are straight since no clusters exist there.

The existence of the clusters was confirmed not only by electron diffraction but also by Lorentz microscopy. Photographic evidence was obtained when we carefully observed the growth of the ferromagnetic domains while gradually decreasing the sample temperature

(Fig. 14). The insulating domains (Fig. 14(a)) began at 54 K to be invaded by ferromagnetic domains (Fig. 14(b)). The invasion was locally interrupted by tiny clusters, resulting in the formation of zigzag domain boundaries. At 45 K, the ferromagnetic domains occupied almost the whole field of view (Fig. 14(c)), and the insulating domains became smaller. The tiny circular domains indicated by the arrows in Fig. 14(c) are attributed to the clusters. At 35 K, the whole field of view was ferromagnetic and conductive.

We also obtained evidence for the effect of magnetic fields on the growth of ferromagnetic domains. Magnetic fields leaking from the ferromagnetic domains, which cannot be observed by Lorentz micrograph (Fig. 15(a)) but by holographic interference micrograph (Fig. 15(b)), help to locally grow the domains.

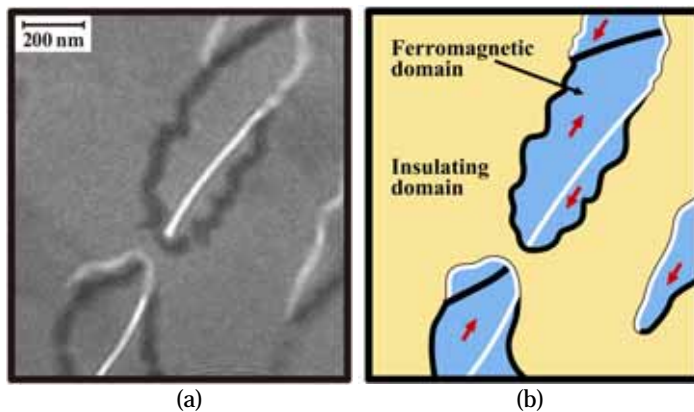


Fig. 13. Coalesced ferromagnetic domains. (a) Lorentz micrograph. (b) Schematic. Boundaries inside ferromagnetic domains are straight, and boundaries between insulating and ferromagnetic domains are zigzag due to existence of charge ordered clusters in insulating domains.

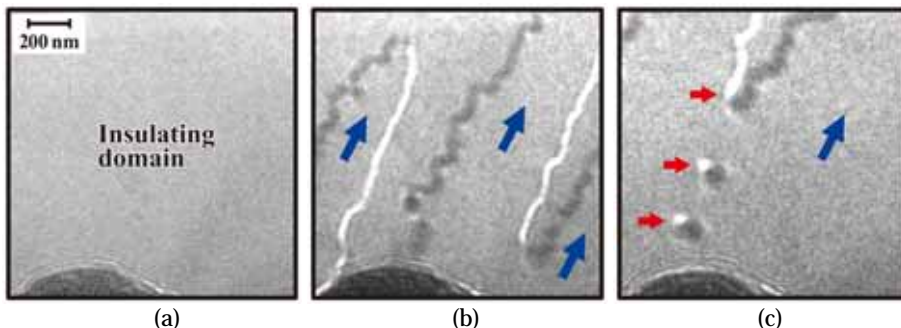


Fig. 14. Evidence of charge-ordered clusters in Lorentz micrographs. (a) $T = 60$ K, (b) 54 K, (c) 45 K. When sample temperature was decreased, ferromagnetic domains grew and finally occupied the whole region, which was insulating at higher temperatures. Tiny circular insulating domains indicated by arrows in (c) were produced at cluster positions. Whole region then became ferromagnetic.

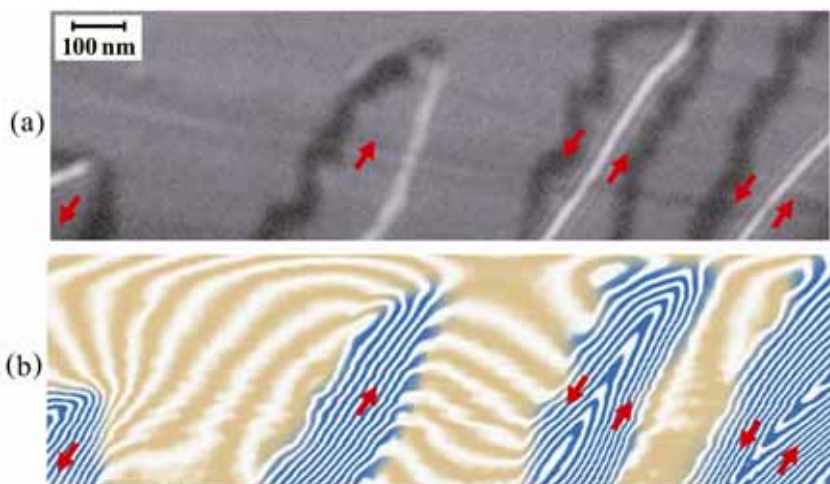


Fig. 15. Growth of ferromagnetic domains in colossal magnetoresistance manganite, $\text{La}_{0.25}\text{Pr}_{0.375}\text{Ca}_{0.375}\text{MnO}_3$, thin film at $T = 62.4$ K. (a) Lorentz micrograph; (b) interference micrograph.

5. Exploring new possibilities

The AB effect celebrated its 50th anniversary in 2009, and symposia on the AB effect were held in Tel Aviv and Bristol. Since the AB effect cannot be understood in terms of classical electrodynamics, a long controversy about it persisted for decades. Even its existence was questioned. Now, however, most physicists regard the AB effect as one of the most fundamental phenomena in quantum mechanics and as related to the deepest concepts of physics. It directly involves the reality of vector potentials, the locality of interactions, the single valuedness of wavefunctions in a multiply-connected space, and so on. Advanced technologies including bright coherent electron beams have made it possible to carry out experiments on the AB effect that were once regarded as thought experiments.

On a personal note, it was the mysterious and yet attractive AB effect in addition to the wave-particle duality of electrons including the theory of observation that motivated me to enter the field of electron wave optics. In 1967, I started research on electron holography, and I had to continually develop brighter, more coherent electron beams. If I had not started this development, the field of electron phase microscopy including electron holography would not be as developed as it is now.

The AB effect was proven to be fundamental to quantum mechanics and also to gauge field theories unifying all fundamental interactions in nature. Therefore, the AB effect is ubiquitous not only in electromagnetism but also in nuclear and gravitational forces. It appears not only in physics but also in chemistry and biology.

In our field of electron microscopy, it has been applied in various ways to the observation of microscopic objects and electromagnetic fields, which are both phase objects for illuminating electrons.

The phase shift of electrons can now be measured with a precision of $1/100$ the wavelength. However, if we want to observe the world of atoms and molecules, this precision is not

enough. We need a precision in the phase measurement of at least the order of 1/1,000 the wavelength, which, I believe, is possible given that the precision approaches 1/10,000 the wavelength of light.

6. References

Aharonov, Y. & Bohm, D. (1959). Significance of Electromagnetic Potentials in Quantum Theory. *Phys. Rev.*, Vol. 115, No. 3, 485-491.

Bocchieri, P. & Loinger, A. (1978). Nonexistence of the Aharonov-Bohm Effect. *Nuovo Cimento A*, Vol. 47, No. 4, 475-482.

Bocchieri, P. & Loinger, A. (1981). Comments on the Letter << On the Aharonov-Bohm Effect >> of Boersch *et al.* *Lett. Nuovo Cimento*, Vol. 30, No. 15, 449-450.

Bocchieri, P.; Loinger, A. & Siragusa, G. (1982). Remarks on << Observation of Aharonov-Bohm Effect by Electron Holography >>. *Lett. Nuovo Cimento*, Vol. 35, No. 11, 370-372.

Boersch, H.; Hamisch, H. & Grohmann, K. (1962). Experimenteller Nachweis der Phasenverschiebung von Elektronenwellen durch das magnetische Vektorpotential. *Z. Phys.*, Vol. 169, No. 2, 263-272.

Chambers, R. G. (1960). Shift of an Electron Interference Pattern by Enclosed Magnetic Flux. *Phys. Rev. Lett.*, Vol. 5, No. 1, 3-5.

Fowler, H. A.; Marton, L.; Simpson, J. A. & Suddeth, J. A. (1961). Electron Interferometer Studies of Iron Whiskers. *J. Appl. Phys.*, Vol. 32, No. 6, 1153-1155.

Gabor, D. (1949). Microscopy by Reconstructed Wave-Fronts, *Proc. R. Soc. Lond. A*, Vol. 197, No. 1051, 454-487.

Hirata, K.; Ishida, Y.; Kim, J. J.; Kasai, H.; Shindo, D.; Takahashi, M. & Tonomura, A. (2009). Electron holography observation of in-plane domain structure in writer pole for perpendicular recording heads. *J. Appl. Phys.*, Vol. 105, No. 7, 07D538-1-07D538-3.

Kim, J. J.; Hirata, K.; Ishida, Y.; Shindo, D.; Takahashi, M. & Tonomura, A. (2008). Magnetic domain observation in writer pole tip for perpendicular recording head by electron holography. *Appl. Phys. Lett.*, Vol. 92, No. 16, 62501-1-62501-3.

Miyazawa, H. (1985). Quantum Mechanics in a Multiply Connected Region. *Proc. 10th Hawaii Conf. High Energy Physics 1985*, Hawaii, Univ of Hawaii, pp. 441-458.

Möllenstedt, G. & Bayh, W. (1962). Kontinuierliche Phasenschiebung von Elektronenwellen im Kraftfeldfreien Raum durch das magnetische Vektorpotential eines Solenoids. *Phys., Bl.*, Vol. 18, 299-305.

Murakami, Y.; Kasai, H.; Kim, J. J.; Mamishin, S.; Shindo, D.; Mori, S. & Tonomura, A. (2009). Ferromagnetic domain nucleation and growth in colossal magnetoresistive manganite. *Nat. Nanotech.*, Vol. 5, No. 1, 37-41.

Osakabe, N.; Yoshida, K.; Horiuchi, Y.; Matsuda, T.; Tanabe, H.; Okuwaki, T.; Endo, J.; Fujiwara, H. & Tonomura, A. (1983). Observation of recorded magnetization pattern by electron holography. *Appl. Phys. Lett.*, Vol. 42, No. 8, 746-748.

Peshkin, M. & Tonomura, A. (1989). "The Aharonov-Bohm effect." *Lecture Notes in Physics*, 340, Springer, 978-3540515678.

Roy, S. M. (1980). Condition for Nonexistence of Aharonov-Bohm Effect. *Phys. Rev. Lett.*, Vol. 44, No. 3, 111-114.

Tonomura, A.; Matsuda, T.; Endo, J.; Arii, T. & Mihamma, K. (1980). Direct observation of fine structure of magnetic domain walls by electron holography. *Phys. Rev. Lett.*, Vol. 44, No. 21, 1430-1433.

Tonomura, A.; Matsuda, T.; Suzuki, R.; Fukuhara, A.; Osakabe, N.; Umezaki, H.; Endo, J.; Shinagawa, K.; Sugita, Y. & Fujiwara, H. (1982). Observation of Aharonov-Bohm effect by electron holography. *Phys. Rev. Lett.*, Vol. 48, No. 21, 1443-1446.

Tonomura, A. (1983). Observation of magnetic domain structure in thin ferromagnetic films by electron holography. *J. Magn. and Magn. Matls.*, Vol. 31-34, Part 2, 963-969.

Tonomura, A.; Umezaki, H.; Matsuda, T.; Osakabe, N.; Endo, J. & Sugita, Y. (1983). Is magnetic flux quantized in a toroidal ferromagnet?. *Phys. Rev. Lett.* Vol. 51, No. 5, 331-334.

Tonomura, A.; Umezaki, H.; Matsuda, T.; Osakabe, N.; Endo, J. & Sugita, Y. (1984). Electron Holography, Aharonov-Bohm Effect and Flux Quantization, In: *Proc. Int. Symp. Foundations of Quantum Mechanics*, edited by Kamefuchi, S.; Ezawa, H.; Murayama, Y.; Namiki, M.; Nomura, S.; Ohnuki, Y. & Yajima, T., Physical Society of Japan, Tokyo, 1984, 20-28.

Tonomura, A.; Osakabe, N.; Matsuda, T.; Kawasaki, T.; Endo, J.; Yano, S. & Yamada, H. (1986). Evidence for Aharonov-Bohm effect with magnetic field completely shielded from electron wave. *Phys. Rev. Lett.*, Vol. 56, No. 8, 792-795.

Tonomura, A. (2005). Direct observation of hitherto unobservable quantum phenomena by using electrons. *Proc. Natl. Acad. Sci. USA*, Vol. 102, No. 42, 14952-14959.

Wu, T. T. & Yang, C. N. (1975). Concept of nonintegrable phase factors and global formulation of gauge fields. *Phys. Rev. D*, Vol. 12, No. 12, 3845-3857.